Effect of Wavy Flow of Vertical Falling Film on the Absorption Performance

Jungkuk Kim, Keumnam Cho*†

Graduate School of Mechanical Engineering, Sungkyunkwan University, Suwon 440-746, Korea

**Department of Mechanical Engineering, Sungkyunkwan University, Suwon 440-746, Korea*

Key words: Absorption performance, Wavy flow, Maximum absorption rate

ABSTRACT: The present study investigated experimentally and numerically the enhancement of absorption performance due to the waviness of falling film in the vertical absorber tube. The momentum, energy and mass diffusion equations were utilized to find out temperature and concentration profiles at both the interfaces of liquid solution and refrigerant vapor and the wall.

Flow visualization was performed to find out the wetting characteristics of the falling film. The maximum heat transfer coefficient was obtained for the wavy flow using spring as an insert device through both numerical and experimental studies. Based on the numerical and experimental results, the maximum absorption rate was found for the wavy-flow using spring as the insert device. The differences between experimental and analytical results ranged from 5.0 to 25% when $\mathrm{Re}_f > 100$.

Nomenclature

A : surface area [m^2]
a : dimensionless film thickness, δ/δ_0
B_0 : local volume flow-rate per unit width [$m^3/m \cdot s$]
C : LiBr solution concentration [wt%]
C_p : constant pressure specific heat [kJ/kg·K]
C_s : concentration of liquid-vapor interface [wt%]
D : mass diffusion coefficient [m^2/s]
d : diameter of absorber tube [m]
d_h : hydraulic diameter [m]
F : fouling factor [$m^2℃/W$]
G : absorption mass flowrate [$kg/m^2 \cdot K$]
h : heat transfer coefficient [$kW/m^2 \cdot K$]
k : thermal conductivity [kW/m·K]
L : length of absorber tube [m]
M : absorption rate [kg/s]
$\dot{m}$: mass flow rate [kg/s]
P : pressure [kPa]
Pr : Prandtl number
q : heat flux [kW/m^2]
$\dot{Q}$: heat flow rate [kW]
r : radius [m]
Re_f : film Reynolds number
Sh : Sherwood number
T : temperature [K]
U : overall heat transfer coefficient [$kW/m^2 \cdot K$]
u : bulk velocity [m/s]
u_0 : specific velocity, B_0/δ_0 [m/s]
We : Weber number
x : flow direction of LiBr solution

Greek symbols

α : dimensionless wave number, δ_0/λ
β : mass transfer coefficient [m/s]
δ : local wave altitude [m]

† Corresponding author
Tel.: +82-31-290-7445; fax: +82-31-290-7923
E-mail address: keumnamcho@skku.edu

δ_0 : mean film thickness [m]
λ : wavelength [m]
μ : viscosity [kg/ms]
ν : kinetic viscosity [m^2/s]
ξ : dimensionless transfer coordinate system
ρ : density [kg/m^3]
σ : surface tension [N/m]
Δ : film thickness per unit length [m]

Subscripts

alt : wave altitude
c : coolant
f : film
i : inside of absorber tube
i, a : interface between LiBr and refrigerant vapor
lm : arithmetic mean
o : outside of absorber tube
ref : refrigerant vapor
s : LiBr solution
ss : stainless steel
w : wall surface of absorber tube
1 : inlet
2 : outlet

1. Introduction

The absorption refrigeration system for the residential space has to be air-cooled, compact, and highly efficient for competing with the vapor compression system. As one of major components affecting the absorption system, an absorber plays an important role the absorption system performance. Especially, the heat and mass transfer in the vertical absorber affects the performance of the absorption refrigeration system. Literatures on the heat and mass transfer characteristics in the vertical absorber are not enough so far. The optimization of an absorber is mainly dependent on the empirical results under the limited experimental conditions and parameters. The performance of the absorption system can be improved by enhancing the absorption performance of the absorber. The energy and diffusion equations were solved by Grossman[1] for laminar films on both isothermal and adiabatic walls. As a function of normalized absorber length, charts for calculation of the Nusselt and Sherwood numbers were produced. A simple model for the absorption of refrigeration vapor into falling films was described by Andberg and Vliet,[2] based on the pre-assumed similarity of the concentration profiles. Non-isothermal absorption wavy laminar films were experimentally characterized by Yueksel and Schluender,[3] and the theoretical predictions agreed with the measured values within ±30%. Patnaik et al.[4] developed design tools for the absorbers with falling films on smooth tubes using NH_3-H_2O and LiBr-H_2O mixtures.

Some experimental and analytical studies on the effect of the absorber geometry on the absorber performance had been performed by Conlisk[5] and Yoon et al.[6] Morioka and Kiyota[7] proposed the optimal thickness of the vertical falling film for the maximum absorption rate of refrigerant vapor. Ohm et al.[8] measured heat and mass transfer coefficients in a vertical copper absorber with the inner diameter of 25 mm for the film Reynolds number from 35 to 150. The absorption performance in the absorber tube may be affected by both the geometric factors such as tube diameter, length, material and the dynamic factors such as solution concentration, solution temperature and pressure, solution flow rate, flow pattern etc. The effect of the flow pattern by the geometric and dynamic parameters on the performance should be analytically and experimentally investigated.

The present study investigated the effect of the falling film flow pattern due to the geometric difference on the absorption performance in a vertical falling film type absorber using LiBr solution with 60 wt%.

2. Modeling and assumptions

A schematic diagram of the falling-film wavy flow on the vertical-tube absorber is shown in Fig. 1. The coolant and LiBr solution are flowing in counter-flow direction, and the entire absorption heat is transferred to the coolant. The solution flows as a falling film on the inner surface of the absorber tube, as concentrated at the top and diluted at the bottom of the tube by absorbing the refrigerant vapor. Numerical solution for the coupled heat and mass transfer equations yields the temperature and concentration profiles.

The system is assumed to be steady-state and two-dimensional. The specific heats of both coolant and LiBr solution are nearly constant, and the heat transfer coefficient on the coolant side of the absorber is assumed to be constant. The falling film is also assumed as a laminar flow. The vapor-side resistance to the mass transfer and the vapor drag on the falling film are negligible.

Based on the above-mentioned assumptions, the simultaneous mass transfer and energy equations at the steady-state are described as Eqs. (1) and (2).

Mass transfer equation;

$$u\frac{\partial C}{\partial x}=D\left\{\frac{\partial^2 C}{\partial x^2}+\frac{1}{r}\frac{\partial C}{\partial r}+\frac{\partial^2 C}{\partial r^2}\right\} \quad (1)$$

Energy equation;

$$\rho c_p\left(u_x\frac{\partial T}{\partial x}+u_x\frac{\partial T}{\partial r}\right)= k\left\{\frac{\partial^2 T}{\partial x^2}+\frac{\partial^2 T}{\partial r^2}\right\}+\frac{\partial}{\partial r}\left(\sum_{i=\mathrm{LiBr}}^{\mathrm{H_2O}}\rho D_i\frac{\partial C_i}{\partial r}h_i\right) \quad (2)$$

where u_x is the bulk velocity in the x-direction of the liquid and refrigerant vapor phases. The properties of LiBr solution and refrigerant vapor are described in Eq. (3).

$$h_{\mathrm{LiBr}}=c_{p,\mathrm{LiBr}}T,\quad h_{\mathrm{H_2O}}=c_{p,\mathrm{H_2O}}T$$
$$C_{\mathrm{H_2O}}=1-C_{\mathrm{LiBr}},\quad D_{\mathrm{LiBr}}=D_{\mathrm{LiBr}}(T) \quad (3)$$

The mass diffusion coefficient is described in Eq. (4) by Reid.[9]

$$D(T)=D(25℃)\left(\frac{T+273.15}{298.15}\right)+\left(\frac{\mu(25℃)}{\mu}\right) \quad (4)$$

$D(25℃)$ and $\mu(25℃)$ are measured data of LiBr solution at 25℃.

The bulk velocity profile is given by

$$u=\frac{3}{2}\bar{u}\left(2\left(\frac{r}{\delta}\right)-\left(\frac{r}{\delta}\right)^2\right) \quad (5)$$

where $\bar{u}$ is the average flow velocity.

For the two-dimensional laminar flow, the unsteady Navier-Stokes equations are shown

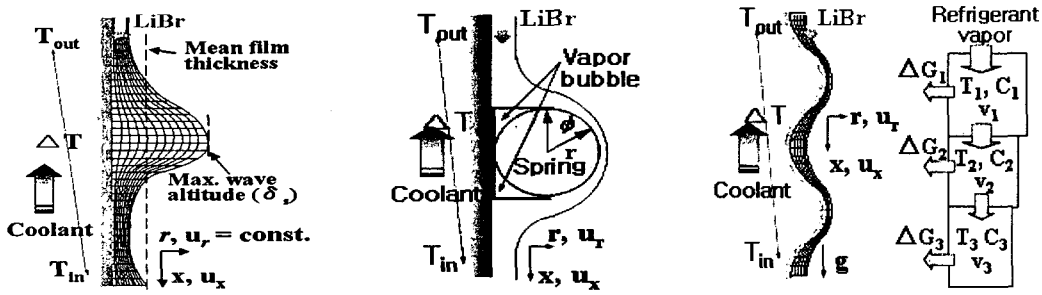

(a) Bare & grooved tube (b) Spring tube (c) Corrugated tube

Fig. 1 Analytical model of a vertical absorber.

in Eqs. (6) and (7) for wavy film flow in the coordinate system in Fig. 1.

$$\frac{\partial u_x}{\partial t}+u_x\frac{\partial u_x}{\partial x}+u_r\frac{\partial u_x}{\partial r}= -\frac{1}{\rho}\frac{\partial p}{\partial x}+g+\nu\left\{\frac{\partial^2 u_x}{\partial x^2}+\frac{\partial^2 u_x}{\partial r^2}\right\} \quad (6)$$

$$\frac{\partial u_r}{\partial t}+u_x\frac{\partial u_r}{\partial x}+u_r\frac{\partial u_r}{\partial r}= -\frac{1}{\rho}\frac{\partial p}{\partial x}+\nu\left\{\frac{\partial^2 u_r}{\partial x^2}+\frac{\partial^2 u_r}{\partial r^2}\right\} \quad (7)$$

Eq. (8) shows dimensionless pressure of LiBr solution and refrigerant vapor.

$$p+ =\frac{p}{\rho U_0^2} \quad (8)$$

The pressure difference of LiBr solution and refrigerant on the vapor-liquid interface is obtained in Eq. (9)

$$(p_{\mathrm{LiBr}}-p_{\mathrm{H_2O}})-\sigma\frac{\partial^2\delta}{\partial x^2}=0 \quad (9)$$

The dimensionless pressure difference is described in Eq. (10)

$$\Delta p+ =-\frac{8a}{\mathrm{Re}}\frac{\partial u_x}{\partial \xi_x}-\frac{a^2}{\mathrm{We}}\frac{\partial^2 a}{\partial \xi_x^2} \quad (10)$$

where Weber number (We) is the ratio of gravity force and surface tension on the LiBr solution and refrigerant surface.

Boundary conditions are shown in Eqs. (11) and (12).

$$C=C_0,\quad T=T_0 \quad \text{at} \quad x=0 \quad (11a)$$

$$\frac{\partial T}{\partial r}=0 \quad \text{and} \quad \frac{\partial C}{\partial r}=0 \quad \text{at} \quad r=rw \quad (11b)$$

$$r=r_1;\ C=f(T,P)$$

$$\dot{q}_s=k\left(\frac{\partial T}{\partial r}\right)-\Delta C_p T\rho D\left(\frac{\partial C}{\partial r}\right) \quad (12)$$

where ΔC_p is the difference of specific heat of solution and coolant at the wall.

The heat transfer rate from solution to coolant is obtained by Eq. (13).

$$\dot{Q}=\dot{m}_c C_{p,c}(T_{c,2}-T_{c,1}) =U_s A_s LMTD \quad (13)$$

The heat flux (q) is obtained by dividing the heat transfer rate in Eq. (13) by the heat transfer area. The overall heat transfer coefficient (U_s) is obtained by Eq. (14).

$$U_s=\frac{1}{\frac{A_i}{A_o}\frac{1}{h_c}+\frac{A_i\ln\left(\frac{r_o}{r_i}\right)}{2\pi k_{ss}L}+\frac{1}{h_s}+F} \quad (14)$$

The fouling factor (F) is 0.00015 $\mathrm{m^2℃/W}$. r_o and r_i are the inner and outer radius of absorber. The convective heat transfer coefficient of coolant, h_c, can be determined by Eq. (15) suggested by Kim et al.,[10] which was for laminar flow in the vertical tube. The heat transfer coefficient of the solution can be obtained by using Eqs. (13)~(15).

$$\mathrm{Nu}_c= \left[\mathrm{Nu}_\infty+f\frac{0.019\left(\mathrm{Re}_c\mathrm{Pr}_c\frac{dh}{L}\right)^{0.8}}{1+0.007\left(\mathrm{Re}_c\mathrm{Pr}_c\frac{dh}{L}\right)^{0.467}}\right]\left(\frac{\mathrm{Pr}_c}{\mathrm{Pr}_w}\right)^{0.11} =\frac{h_c d_c}{k_c} \quad (15)$$

According to the uncertainty analysis suggested by Moffat[11] in Eq. (16), the heat transfer coefficient has the error range from ±1.2 to ±3.1%.

$$\frac{\delta h_s}{h_s}=\sqrt{\left[\frac{\delta\dot{Q}}{\dot{Q}}\right]^2+\left[\frac{\delta A}{A}\right]^2+\left[\frac{\delta T_{s,1}}{\Delta T_{lm}}\right]^2+\left[\frac{\delta T_{s,2}}{\Delta T_{lm}}\right]^2} \quad (16)$$

The absorption mass flow-rate is shown by

$$\dot{G} = \frac{M}{A_i} = \dot{m}_s\left(\frac{C_{s,1}}{C_{s,2}} - 1\right) \tag{17}$$

The mass transfer at a falling film is obtained by the difference between the solution concentration at the liquid-vapor interface and average concentration of the falling film. Since the solution concentration at liquid-vapor interface cannot be measured, it can be replaced by the saturated concentration at the pressure of the absorber and the solution temperature. The absorption rate of refrigerant vapor is given by Eq. (18).

$$M = \rho_s \beta A_{i,a} \Delta C_{lm} \tag{18}$$

The mass transfer coefficient can be calculated by Eqs. (17) and (18).

According to the uncertainty analysis in Eq. (19), the absorption rate showed the error range from ±1.7 to ±3.6%.

$$\frac{\delta G_s}{G_s} = \sqrt{\left[\frac{\delta\rho_s}{\rho_s}\right]^2 + \left[\frac{\delta\beta}{\beta}\right]^2 + \left[\frac{\delta C_{s,1}}{\Delta C_{lm}}\right]^2 + \left[\frac{\delta C_{s,2}}{\Delta C_{lm}}\right]^2} \tag{19}$$

3. Experimental apparatus and conditions

Figure 2 shows the schematic diagram of the present experimental system, which consists of an absorber, a generator, a solution tank, an evaporator, a condenser, a constant temperature bath, a mass flow meter and a sampling device.

The absorber consists of an upper header, an absorbing tube and a lower header. The absorber tubes with the thickness of 1 mm were made of stainless steel tube (SUS316). The LiBr-H_2O solution flows downward in parallel to the gravity from the upper header to the absorbing tube. Then, it turned to the weak solution after the absorption process. It moves toward the lower header of the absorber and then to the solution tank. Thermocouples were installed at the upper and lower headers to measure the temperatures of both strong and weak solutions. The coolant temperatures were also measured at the inlet and outlet of the coolant channel. T-type thermocouples with the diameter of 0.0762 mm were used. The pressures at the inlet and outlet of the absorber were measured by an absolute pressure gauge. The strong solution in the generator and weak solution at the outlet of the absorber were extracted by using a sampling trap. Its specific gravity was measured by a volumetric flask of 25 ml and an electronic balance with the accuracy of ±0.1 mg. The magnetic solution pump with a capacity of 0.033 kg/s was used to cir-

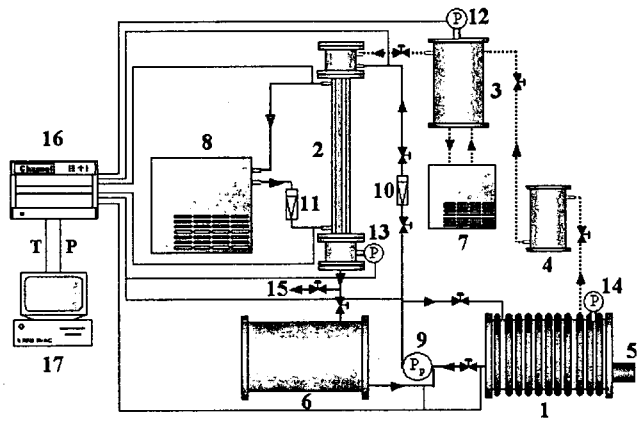

1. Generator
2. Absorber
3. Evaporator
4. Condenser
5. Heater
6. Weak solution tank
7~8. Constant temp. bath
9. Magnetic pump
10~11. Rotameter
12~14. Vacuum pressure gage
15. Sampling trap
16. Data acquisition board
17. PC

Fig. 2 Schematic diagram of the present experimental apparatus.

(a) Bare tube (b) Grooved tube (c) spring tube

Fig. 3 Photographs of flow pattern (Re_f=90).

culate the solution into the absorber.

The geometric parameters of the heat and mass transfer characteristics by the falling-film flow pattern in a vertical absorber are the shape of the absorber such as bare tube, grooved tube and spring tube. The dynamic parameters are the film Reynolds numbers from 30 to 150. The pressure in the absorber was set as 1.01 kPa, and the flow rate of the cooling water was fixed at 0.025 kg/s.

Figure 3 shows the film flow pattern for different shapes of absorber tube. Film separation and flow instability in bare tube increased as the roughness of wall surface increased. But the micro-grooved and spring tubes in Fig. 3 (b) and (c) showed the uniform film due to the increase of the frictional force between LiBr-solution and absorber wall.

The present study has been carried out under the following conditions; inlet concentration of LiBr solution ($C_{s,1}$) of 60 wt%, inlet solution temperature ($T_{s,1}$) of 45℃, inlet coolant temperature ($T_{c,1}$) of 30℃, pressure of refrigerant vapor (P_{ref}) of 7.6 mmHg and film Reynolds number from 30 to 160.

4. Results and discussion

Figure 4 shows the maximum wave altitude and maximum film thickness with respect to the wave length in the numerical analysis. The maximum wave altitude for λ smaller than 0.02 m was decreased rapidly. The maximum wave altitude for λ>0.02 m was predicted as 0.318 mm due to the increase of the frictional force between LiBr-H_2O solution and absorber wall.

The maximum wavy film thicknesses of periodic wave for λ larger than 0.02 m was higher by 2.2~3.0% than those of mean film thickness of uniform film, the effect of the wave length on the wave altitude showed similar trend.

Figure 5 shows the maximum heat transfer coefficient and the effect of local vapor bubble with respect to the wavy flow by the spring. The maximum heat transfer coefficient was predicted at the upper end and lower end of the spring with constant concentration and temperature of LiBr solution. The maximum heat transfer coefficient at upper end of respective spring was increased by 30.7% due to the increase of thermal resistance by the local vapor bubble among LiBr-H_2O solution, absorber wall

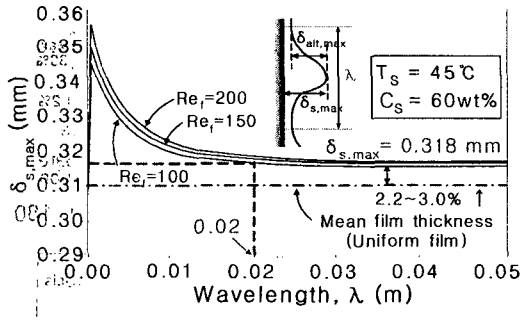

Fig. 4 Effect of λ on maximum wave altitude for a bare tube.

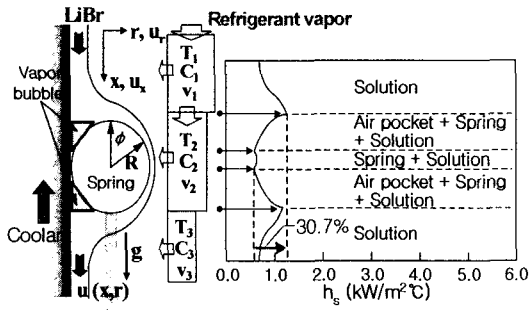

Fig. 5 Heat transfer characteristics for a spring tube.

and spring as shown in Fig. 5.

The heat transfer coefficient at the middle of respective spring was decreased by maximum 30.7% than those for the upper end of spring. The effect of the local vapor bubble on the absorption performance showed similar trend within operating Reynolds number.

Figure 6 shows the heat transfer coefficients with respect to the film Reynolds numbers from 30 to 160 for different wavy film flow pattern.

The heat transfer coefficients on the wavy film flow of bare tube were increased by 0.7~6.5% compared to those of the uniform film. Heat transfer coefficients for the spring tube were increased by the maximum of 15% compared to those of the bare tube, and they were large in the order of bare, grooved, corrugated and spring tubes.

The analytical results were 12.5~25% greater than the experimental data due to the assumptions for numerical analysis. The measured heat transfer coefficients were decreased due to the decrease of the local heat transfer area caused by the instability of film flow and the increase of local thermal resistance.

As the film Reynolds number increased, the film shape became uniform and stable, and the absorption resistance of refrigeration vapor due to the instability of film flow decreased. The mass transfer rate increased due to the increase of heat transfer area and absorbing area. The total heat transfer rate increased by the sensible heat as the mass transfer rate increased. The heat transfer coefficients were large in the reverse order of uniform film, wavy film and rapidly wavy flow in the tube with spring.

The heat transfer coefficients solved by Grossman et al.[1] were higher than those by the present study at the Ref less than 90 due to the assumed uniform film and constant temperature at the wall.

The part of falling film of the solution was separated due to the roughness of wall surface. As the heat transfer area decreased due to the non-wetting area, the local thermal resistance increased and the heat transfer coefficient decreased.

Figure 7 shows the variation of the absorption mass flux with respect to the film Reynolds numbers for wavy film flow pattern in the absorber. The absorption mass flux was significantly increased up to the film Reynolds number of 90, peaked on it, and then remained constant. The enhancements of absorption mass

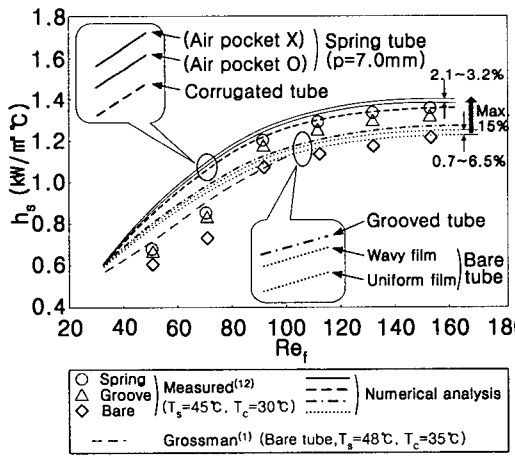

Fig. 6 Effect of surface shape on h_s.

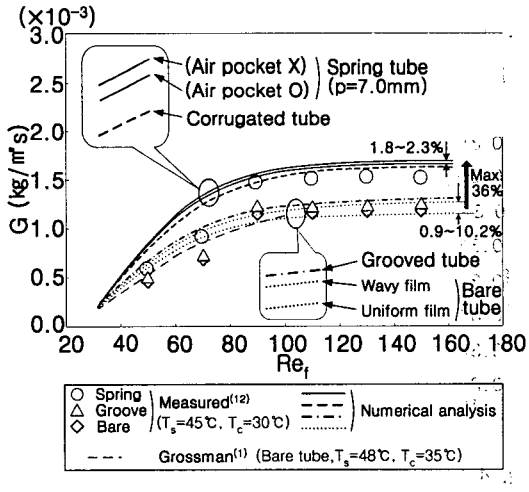

Fig. 7 Effect of surface shape on G.

flux by the wavy flow pattern for $Re_f>90$ were larger than those for $Re_f<90$.

The absorption mass fluxes of the bare tube for the wavy film flow increased by 0.9~10.2% compared to those for uniform film.

As the rapidly wavy flow for spring tube became the uniform and stable, the absorption mass fluxes for spring tube increased by the maximum of 36% than those of the bare tube. Mass transfer showed similar trend with heat transfer. The absorption mass flux was large in the order of bare, grooved, corrugated and spring tubes.

Numerical results by Grossman et al.[1] were higher by the maximum of 16.6% than those by the present study at $Re_f>90$. The differences from the data by Grossman et al.[1] were caused due to the simplified assumptions such as constant temperature of wall, constant diffusion coefficient and uniform film flow. They led to the increase of absorption performance as compared with the present study.

The diffusion coefficient at the outlet of absorber decreased due to the decrease of concentration by the absorption of refrigerant vapor in the absorber, and the measured temperature of wall of absorber increased by the heat flux between LiBr-H_2O solution and coolant. The constant diffusion coefficient of the solution led to large absorption rates, and the constant temperature of coolant caused the increase of the absorption rates.

The numerical results were larger by 5~15 % than the experimental results. The differences were due to flow instability and increase of local thermal resistance by local non-wetting.

5. Conclusions

The present study can be summarized as follows;

(1) The maximum wave altitude for $\lambda>0.02$ m was predicted as 0.318 mm due to the increase of the frictional force between LiBr-H_2O solution and absorber wall.

(2) The maximum film thickness of the wavy flow was higher by 2.2~3.0% than that of uniform film. The effect of wavelength on the wave altitude showed similar trend within operating Reynolds numbers.

(3) The absorption mass flux and heat transfer coefficients increased due to the wavy film. The heat transfer coefficient and the absorption mass fluxes of the bare tube for the wavy film flow increased by the maximum of 6.5, 10.2% respectively than those for uniform film.

(4) The heat and mass transfers were large in the order of bare tube, grooved, corrugated and spring tube. Heat transfer coefficient and absorption mass flux for the spring tube were increased by the maximum of 15, 36% respectively than those for the bare tube.

(5) As the instability of film flow increased, the numerical values were getting larger than the measured data. The differences of experimental and analytical results were ranged within 5~25%.

Acknowledgement

This work was supported by grant No. 2005-E-BD11-P-05-3-010-2005 from the Korea Energy Management Corporation and the Brain Korea 21 project (2005).

References

1. Grossman, G., 1983, Simultaneous heat and mass transfer in film absorption under laminar flow, Int. J. Heat and Mass Transfer, Vol. 26, No. 3, pp. 357-371.
2. Andberg, J. W. and Vliet, G. C., 1983, Design guidelines for water-lithium bromide absorbers, ASHRAE Transactions, Vol. 89, No. 1B, pp. 220-232.
3. Yueksel, I. and Schluender, W., 1988, A model of an Ammonia-water falling film absorber, ASHRAE Transactions, Vol. 94,

No. 1, pp. 467-483.
4. Patnaik, V., Perez-Blanco, H. and Miller, W. A., 1992, Experimental validation of a simple analytical model for the desing of vertical tube absorbers, In progress.
5. Conlisk, A. T., 1995, Analytical solution for the heat and mass transfer in a falling film absorber, Chemical Engineering Science, Vol. 50, No. 4, pp. 651-660.
6. Yoon, J. I., Oh, H. K. and Kashiwagi, T., 1995, Characteristics of heat and mass transfer for a falling film type absorber with insert spring tubes, Transaction of KSME, Vol. 19, No. 6, pp. 1501-1509.
7. Morioka, I. and Kiyota, M., 1987, Absorption of water vapor into a lithium-bromide water solution film falling along a vertical plate, Transactions of the JSME (Part B), Vol. 53, No. 485, pp. 236-240.
8. Ohm, K. C., Kashiwagi, T. and Seo, J. Y., 1993, Characteristics of absorption and heat transfer for film falling along a vertical inner tube (characteristics of absorption), Korean Journal of Air-Conditioning and Refrigeration Engineering, Vol. 5, No. 1, pp. 1-9.
9. Reid, R., 1977, The properties of gases and liquids, McGraw-Hill, New York Press, pp. 31-36.
10. Kim, K. J., Berman, N. S. and Wood, B. D., 1995, Absorption of water vapor into falling films of aqueous lithium bromide, Int. J. Refrigeration, Vol. 18, No. 7, pp. 486-494.
11. Moffat, R. J., 1985, Using uncertainty analysis in the planning of an experiment, Trans. of the ASME: J. of Fluid Engineering, Vol. 107, pp. 173-182.
12. Kim, J. K. and Cho, K., 2002. Analytical and experimental study on the absorption performance in the vertical absorber, Proceeding of the 7th International Sorption Heat Pump Conference, pp. 315-319.